

1 **SUPPLEMENTARY INFORMATION**

2

3 **A semi-quantitative visual lateral flow immunoassay for SARS-CoV-2 antibody**
4 **detection: a strategic tool for the follow-up of immune response after vaccination**
5 **and recovery**

6 Simone Cavalera^a, Fabio Di Nardo^{a*}, Thea Serra^a, Valentina Testa^a, Claudio Baggiani^a, Sergio Rosati^b, Barbara
7 Colitti^b, Ludovica Brienza^b, Irene Colasanto^b, Chiara Nogarol^c, Domenico Cosseddu^d, Cristina Guiotto^d, Laura
8 Anfossi^a

9 ^a Department of Chemistry, University of Turin, Via Pietro Giuria 7, Turin, Italy

10 ^b Department of Veterinary Science, University of Turin, Largo Braccini 2, Grugliasco (TO), Italy

11 ^c In3diagnostic srl, Largo Braccini 2, Grugliasco (TO), Italy

12 ^d A.O. Ordine Mauriziano, Ospedale Umberto I di Torino, Via Magellano 1, Turin, Italy

13 *e-mail: fabio.dinardo@unito.it*

14

15 **Index**

16

17 **S1. Salt-induced aggregation test**2

18 **S2. Gold conjugate synthesis**2

19 **S3. Optimization of the three serological LFIA device for format selection by design of experiments**2

20 **S4 Characterisation the AuNPs conjugates**3

21 **FIGURES**4

22 **TABLES**16

23 **References**24

24

25

26 *S1. Salt-induced aggregation test*

27 To define the minimum amount of protein stabilizing AuNP, the salt-induced aggregation test was applied.
28 250 μL of AuNP solution at optical density 1 were inserted in wells of a microtiter plate and incubated at 37°C
29 for 30 min with increasing amounts (0-0.5-1.0-1.5-2.0-2.5 μg) of the protein. The solution of AuNPs was
30 previously adjusted to an optimal pH for the conjugation. Typically, a pH higher than the isoelectric point is
31 used to promote protein adsorption. In the case of the Spike protein, the pI is reported between 7-8[1]. For
32 the SpA the pI is lower and, most important, the SpA was reported as lowly stable at pH above 7.5. For these
33 reasons, the stress test was performed at pH 8 for cSp, nSp, and anti-hlgG, while it was carried at pH6 for
34 SpA[2]. Then, 25 μL of aqueous NaCl (10% w/v) was added and reacted for 10 min to promote aggregation
35 of unstable AuNPs. The absorbance of the solutions was read at 540 and 620 nm by a microplate reader
36 (Multiskan FC, Microplate Photometer) and the ratio of the two values was calculated and plotted towards
37 the quantity of the protein added (**Figure S3**). The stabilizing amount was defined as the lowest one providing
38 the high and stable absorbance ratio and was approximately the same for cSp and SpA (2 μg), while it was 10
39 μg for the anti-hlgG. The nSp presented a slightly higher stabilizing amount (4 μg) but, for comparing with
40 the cSp, it was tested in the DoE with the same amounts used for cSp.

41 *S2. Gold conjugate synthesis*

42 In order to optimize the gold conjugate employed in the LFIA's development, the best combination of protein-
43 to-AuNP ratio and the optimal optical density of the conjugate to be included into the device were explored.
44 Three gold conjugates were employed for the LFIA-1 strategy using the cSp (AuNP-cSp). Basing on the result
45 from the salt-induced aggregation test (**Figure S4**), the minimum amount of cSp stabilizing the AuNPs from
46 aggregation was 2 μg . Then amounts of 1-2-4 μg were used, corresponding to the 0.5-1-2x of the minimum
47 stabilizing amount. The same was done for the nSp, despite the stabilization was reached with 4 μg , for
48 comparing the two differently produced proteins. The same considerations were made for the conjugation
49 of the anti-hlgG antibody for the LFIA-3 strategy, with 5-10-15 μg adsorbed onto AuNPs. The AuNP-SpA was
50 similarly optimized, firstly with 0.2-0.5-1-2-4-6 μg , corresponding to 0.1-0.25-0.5-1-2-3x of the stabilizing
51 amount. The wider ranges of concentration explored was chosen considering from one hand the high
52 capacity (5 binding domains) of this bioligand and, on the other hand the possible occupation of binding sites
53 by non-specific immunoglobulins, which could reduce the bioligand effectively available for the recognition
54 of specific antibodies. The gold conjugates used in the LFIA's were prepared by coating the surface of the
55 AuNPs with different proteins by passive adsorption. In detail, 1 mL of AuNPs solution at optical density of ca
56 1 was adjusted to pH 8 by adding carbonate buffer, 50 mM pH 9.6. An amount of protein dissolved in aqueous
57 buffer (typically phosphate 20 mM pH 7.4, or milliQ water) was added and the mixture was incubated 30
58 minutes at 37°C. Then a non-specific protein (BSA) dissolved in borate buffer 20 mM, pH 8, was added to
59 stabilise the resulting gold conjugates, which were recovered by centrifugation (15000xg, 12 min) and
60 washed twice with borate buffer supplemented with 0.1% BSA. Finally, the gold conjugates were re-
61 suspended in probe storage buffer (borate buffer 20mM, pH 8, with 1% BSA, 0.25% Tween 20, 2% sucrose,
62 and 0.02% sodium azide) and stored at 4 °C until use. AuNP-SpA gold conjugates were prepared at pH 6 in
63 the adsorption step, and at pH 7.4 in the washing and storing buffers, with the same additives used in the
64 basic buffers.

65

66 *S3. Optimization of the three serological LFIA device by design of* 67 *experiments*

68 Full-factorial (FF-DoE) and D-optimal designs of experiments were performed to define the most sensitive
69 gold conjugates for each of the three qualitative LFIA formats investigated.

70 The intensity of the colour was measured on the test line upon applying the same high positive serum (#1001,
71 5680 AU mL⁻¹) for all the experiments. Each condition was double tested, and the intensity of the colour was
72 plotted against the optical density of the gold conjugate (which relates to the amount of the detector) and
73 against the protein-to-AuNP ratio. The LFIA-1 format, based on the double-antigen strategy, was tested with
74 three gold conjugates differing for the amount of the protein adsorbed onto AuNP (with 1, 2, and 4 µg), each
75 applied at three different optical densities (2,3, and 4), for a total of 9 conditions (FF-DoE). The LFIA-1 strategy
76 was explored both with cSp and with the nSp. The LFIA-2 format, based on the use of the bacterial ligand
77 SpA, was studied first by incorporating four gold conjugates (with 1, 2, 4, and 6 µg adsorbed onto AuNP),
78 applied at four optical densities (2,3, 4, and 5), for a total of 16 conditions, cut down to 9 by D-optimal. A
79 further extension of the DoE included 0.2, 0.5, and 1 µg adsorbed onto AuNP and optical density of 5, 7, and
80 9 (9 experiments FF-DoE). The LFIA-3 format, based on the use of the anti-human IgG secondary antibody,
81 was studied first with three gold conjugates (characterized by 5, 10, and 15 µg adsorbed onto AuNP),
82 combined with three optical densities (2, 3, and 4), for a total of 9 conditions (FF-DoE). A further extension
83 of the DoE included optical density of 5, and 6 combined with 10 and 15 µg adsorbed onto AuNP (4
84 experiments FF-DoE). The best conditions were defined as satisfying requirements of the highest colour
85 intensity of the test line for the positive control and absence of colour for the negative control.

86 *S4 Characterisation of the AuNPs conjugates*

87 Gold conjugates were analysed by means of a Cary 60 UV-Visible spectrophotometer (Agilent, Santa Clara,
88 CA, USA) in the UV-visible range (**Figure S3**) and maximum of the localised surface plasmon resonance (LSPR)
89 band was extracted by first derivative of the experimental data. All conjugates were characterized by a red
90 shift of the wavelength of the maximum of the localized surface plasmonic resonance band (λ_{\max} LSPR)
91 compared to the one of bare AuNPs. The shift was considered as a confirmation of their successful adsorption
92 (**Table S1**), as due to the formation of the protein layer onto gold nanoparticles. The extent of the shift
93 depended on the nature (and partially on the amount of the protein) used. The cSp and nSp added between
94 1 µg and 4 µg, induced a λ_{\max} LSPR shift of 1.0-3.6 nm, while SpA, from 0.2 µg up to 6 µg induced a less
95 significant shift (0.1-1.4 nm). The anti-hIgG antibody (added in the amounts comprise between 5-15 µg)
96 caused a large λ_{\max} LSPR shift (5.4-6.9 nm) with limited dependency on the amount of antibody, suggesting
97 competing phenomena to saturation of the surface or a limited dependence of the plasmonic resonance on
98 antibody amount above a threshold.

99

100

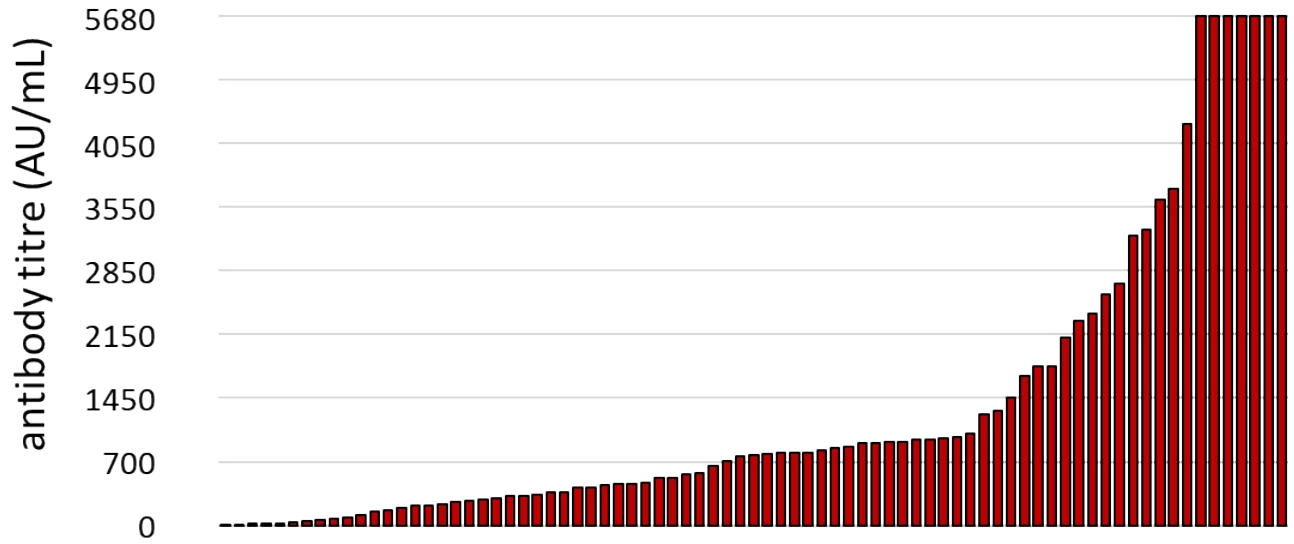
101

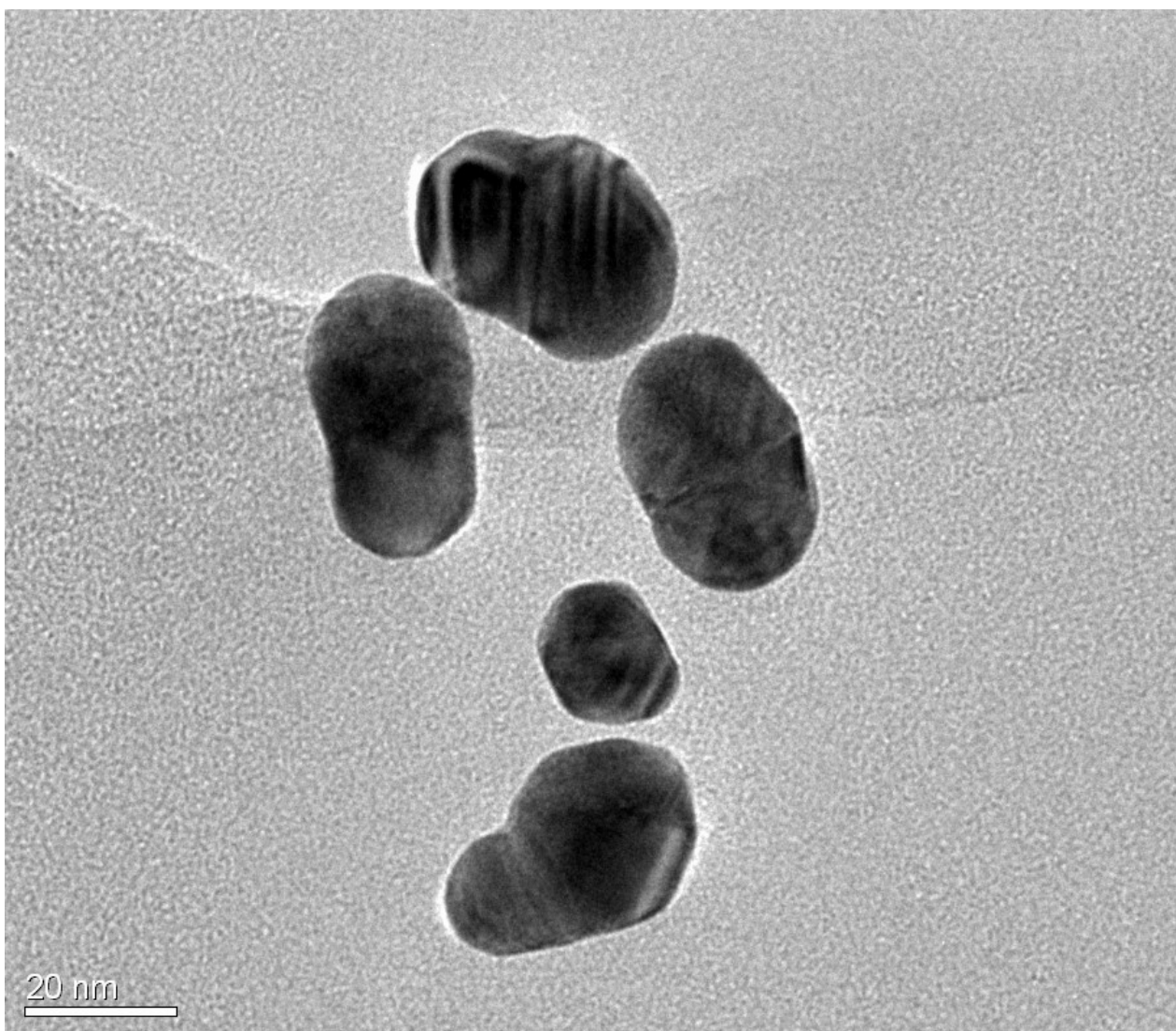
102

103 **FIGURES**

104

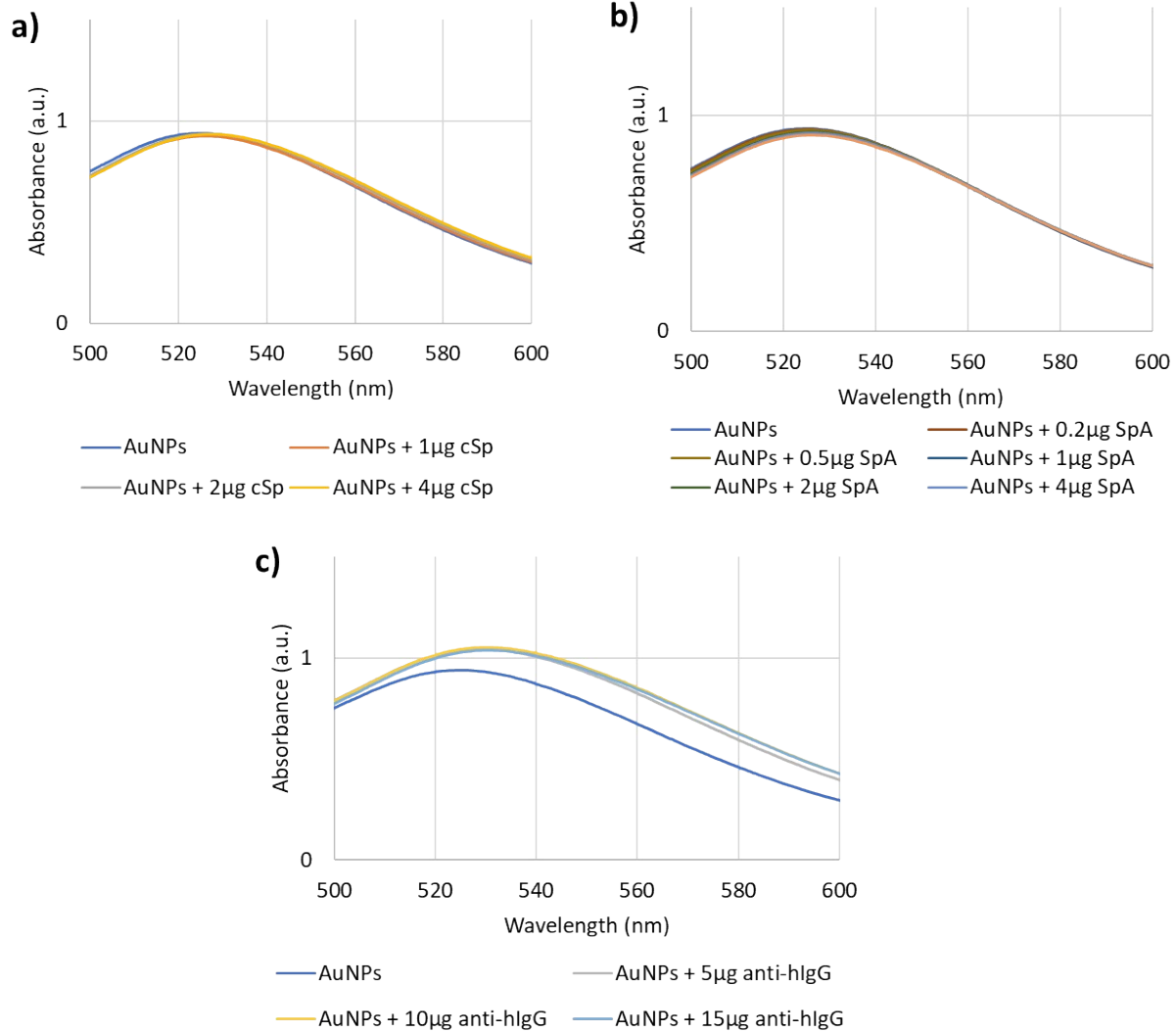
105





110

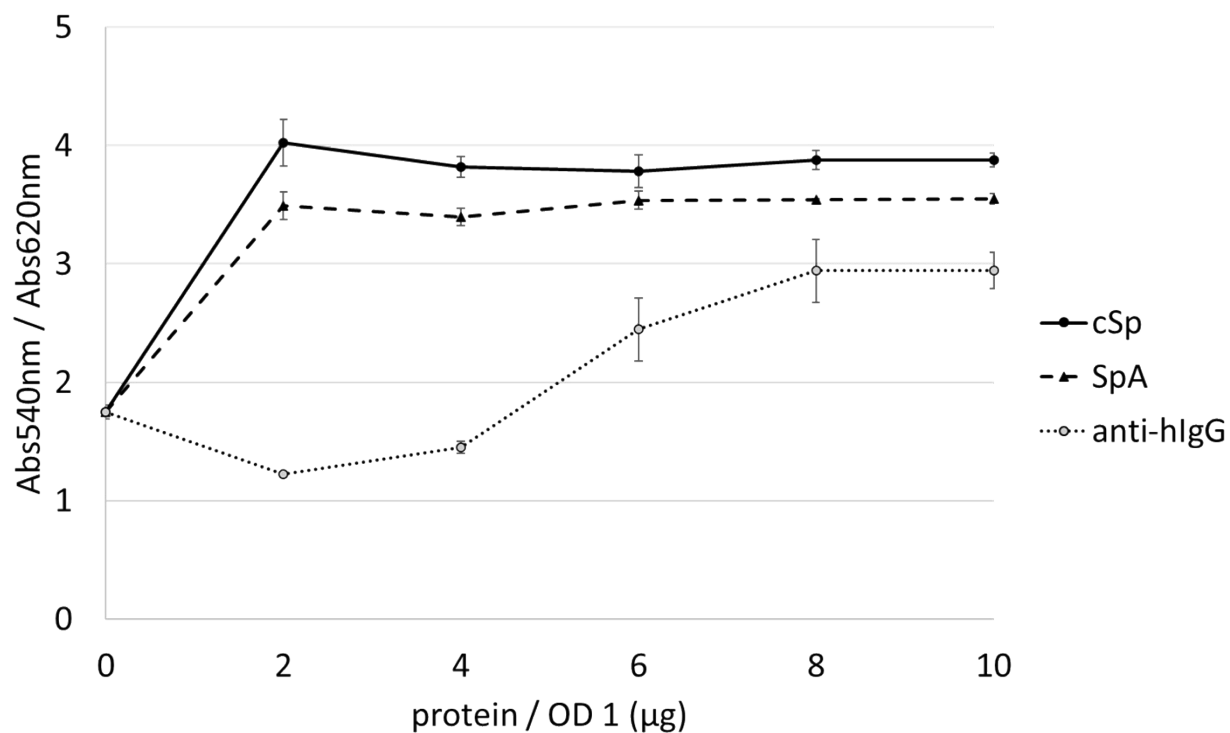
111 **Figure S2:** TEM images of 30nm AuNPs obtained in this work.



112

113 **Figure S3:** Visible spectra of the gold nanoparticles conjugated to various proteins: cSp (a), nSp (b), SpA (c),
 114 and anti-hlgG (d). Different quantities of each protein were added, to prepare conjugates used in the DoE.

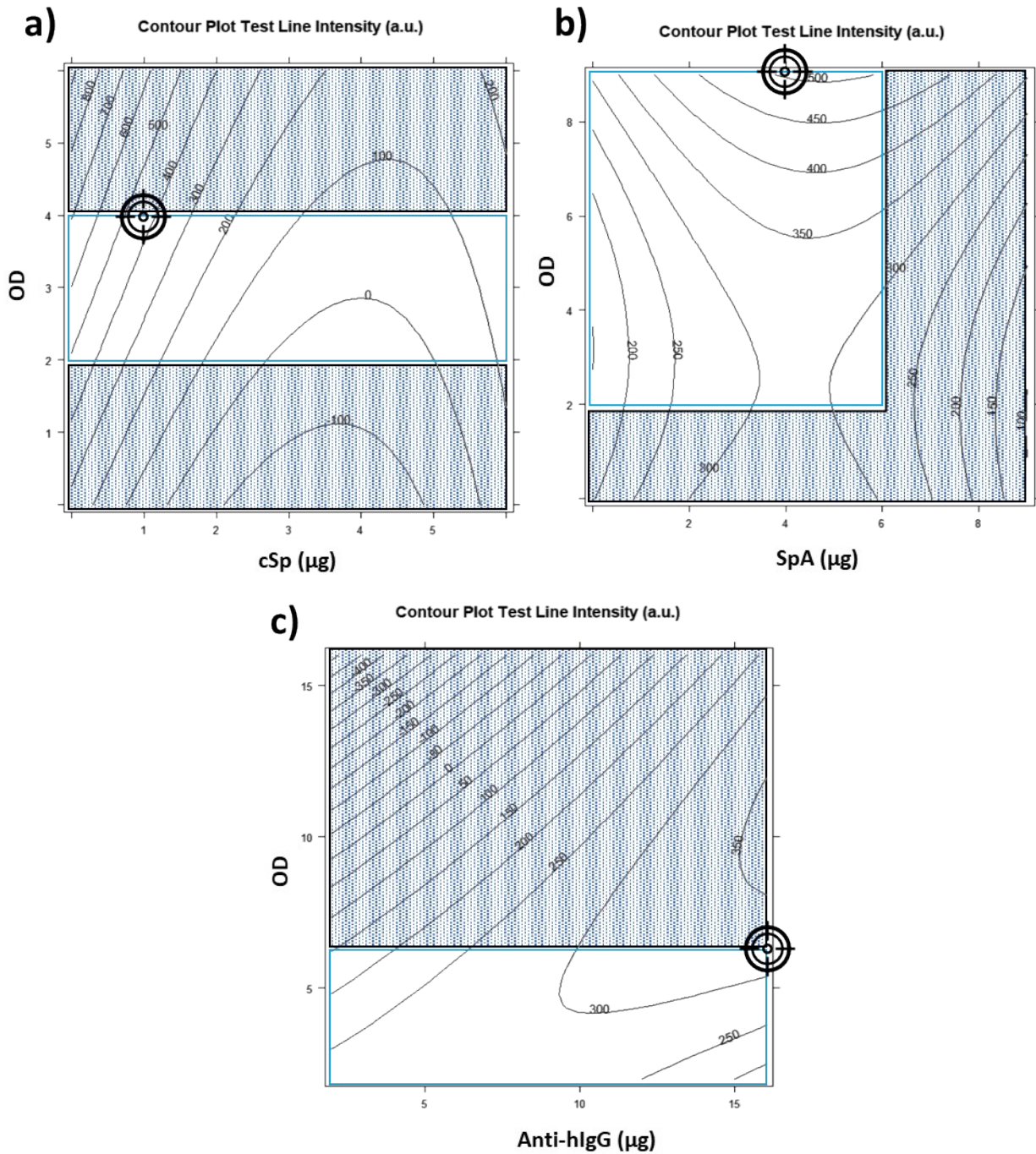
115



117

118 **Figure S4:** The results from the salt-induced aggregation test for cSp, nSp, SpA and anti-hlgG secondary
 119 antibody on AuNPs. The absorbance ratio (540/620) above 4 was considered as corresponding to AuNPs
 120 completely shielded by the protein[3] and the lower protein content corresponding to Abs540/Abs620 > 4
 121 was used as the reference amount to set the levels of the DoE.

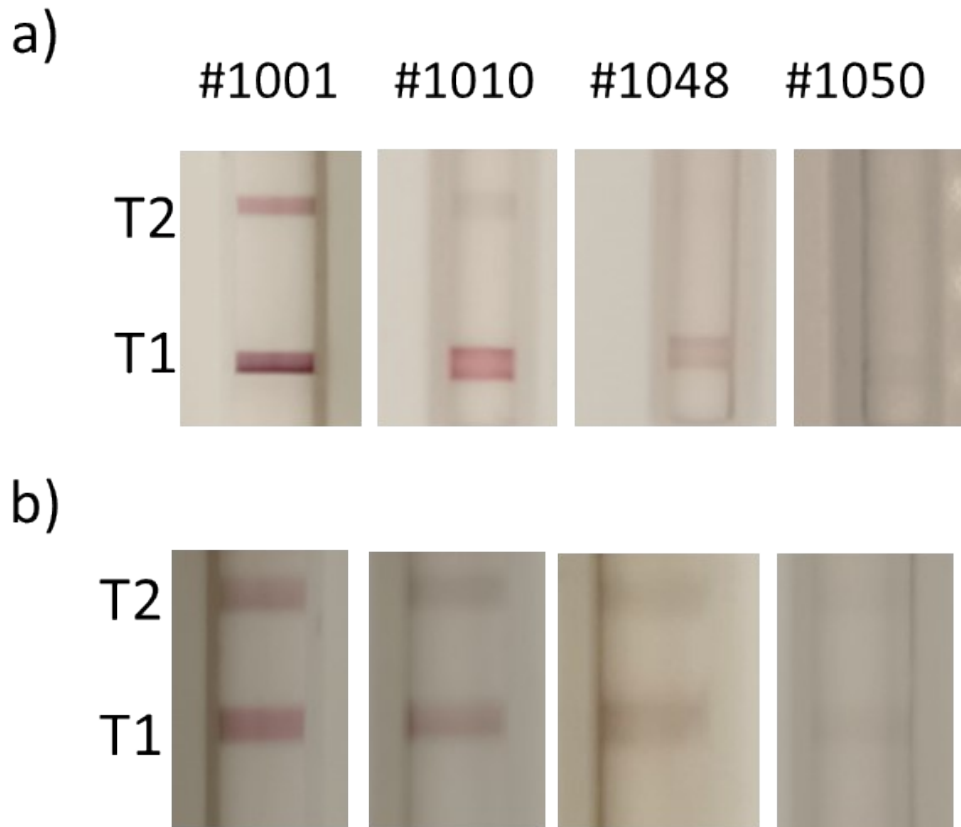
122



123

124 **Figure S5:** The results from the design of experiments for the decision on the gold conjugates parameters
 125 (protein and optical density) for the recombinant RBD (a), the SpA (b), and the anti-human IgG antibody (c).
 126 The bull's-eye refers to the probe chosen for the development of the LFIA devices. Blue shaded zones are
 127 unexplored experimental space.

128

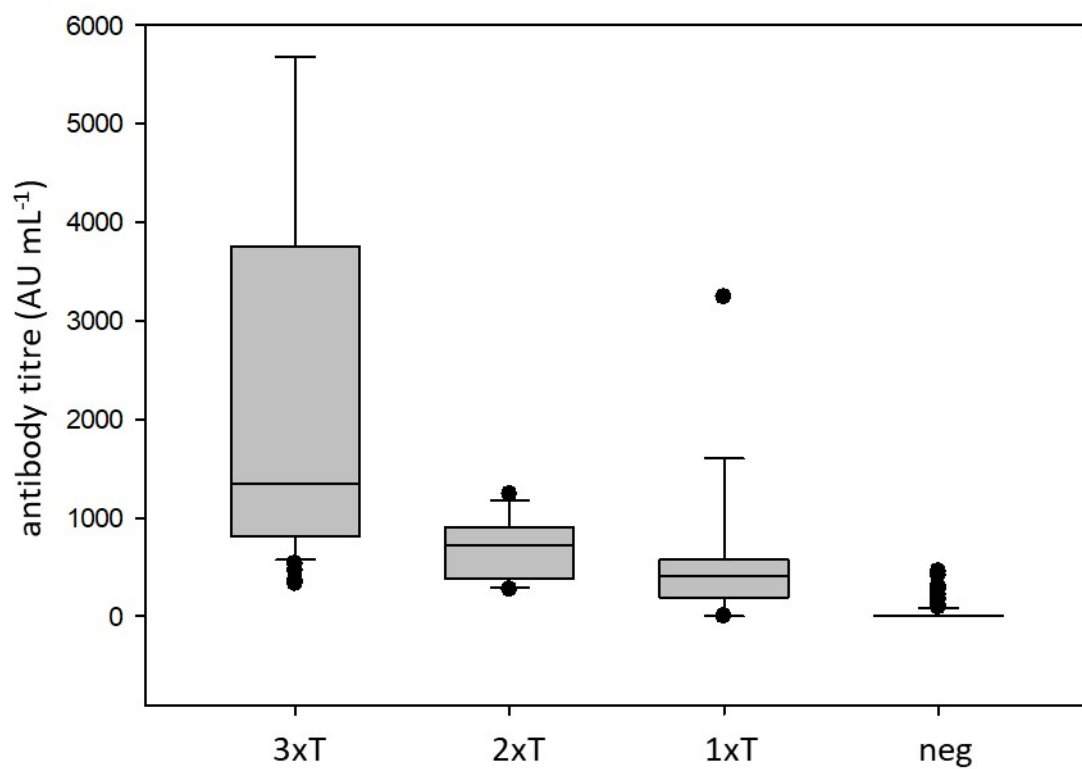


129

130 **Figure S6:** Examples of tuning the concentration of the capture protein that formed the second test line (T2)
 131 in the sqLFIA. By using the double antigen approach (a), two lines were visible for the high-titre (#1001) and
 132 medium-high (#1010) samples, while the medium-low-titre and low (#1048 and #1050) gave just one test
 133 line response. On the contrary, when using the SpA as the detector ligand (b), the intensity of the colour of
 134 the two test lines was comparable among the medium-low-titre positive serum (#1048) and the high- and
 135 medium-high titre sera (#1001 and #1010), so no discrimination among these levels was possible.

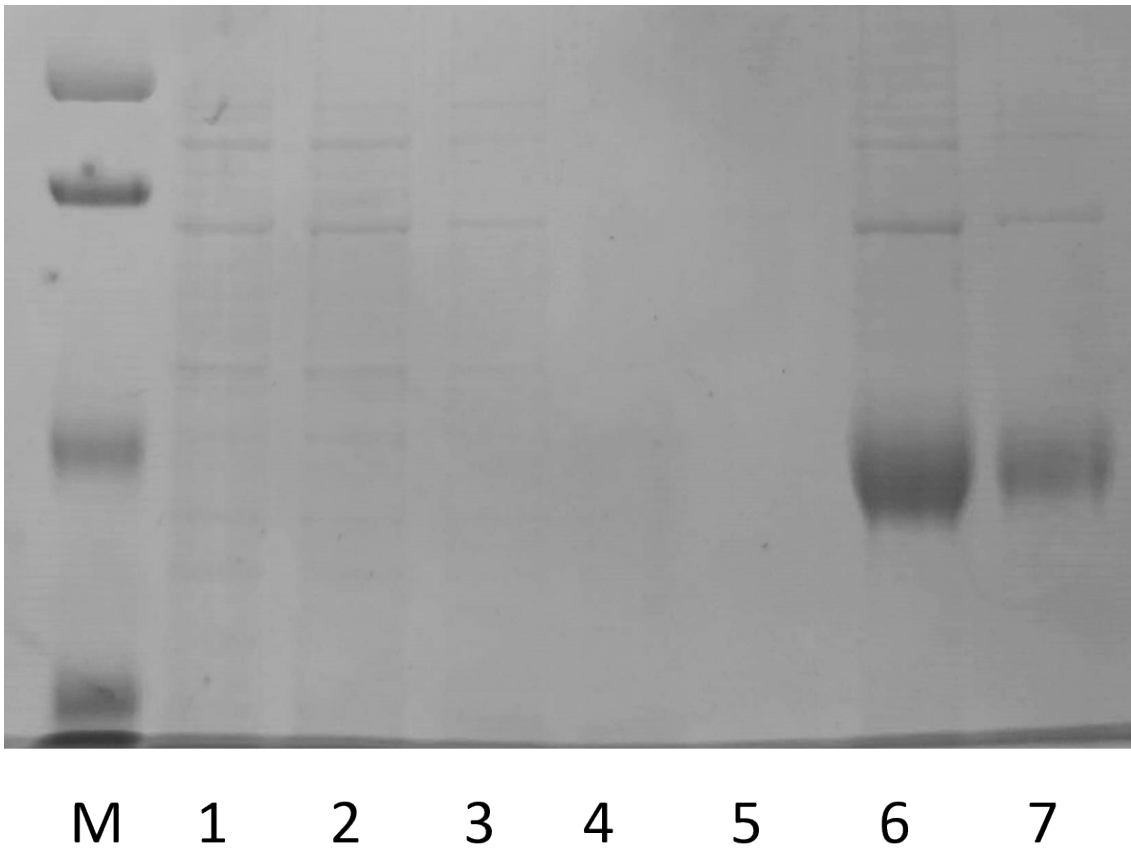
136

137



138
139 **Figure S7:** Box plot obtained by testing the 171 samples by the three-test-line sqLFIA prototype.
140
141

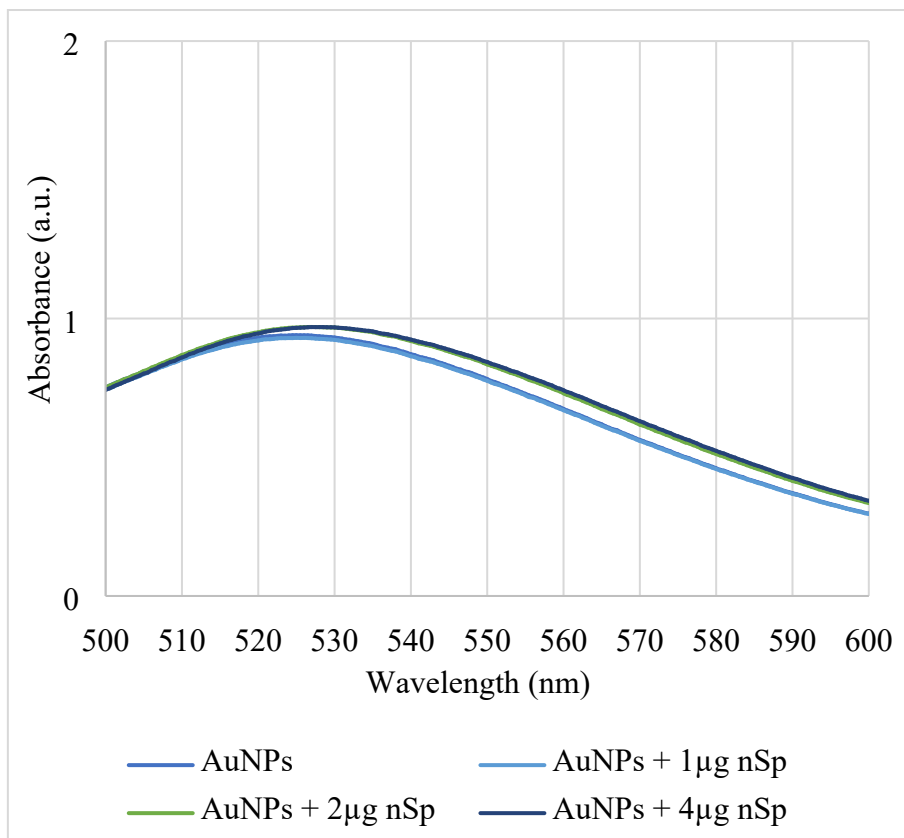
142



143

144 **Figure S8:** SDS-PAGE showing expression and purification of recombinant RBD in mammalian cells. M,
145 molecular weight standard; 1, culture supernatant 5 days p.t.; 2, flow through; 3-4, wash, 5-6-7, eluted
146 fractions.

147



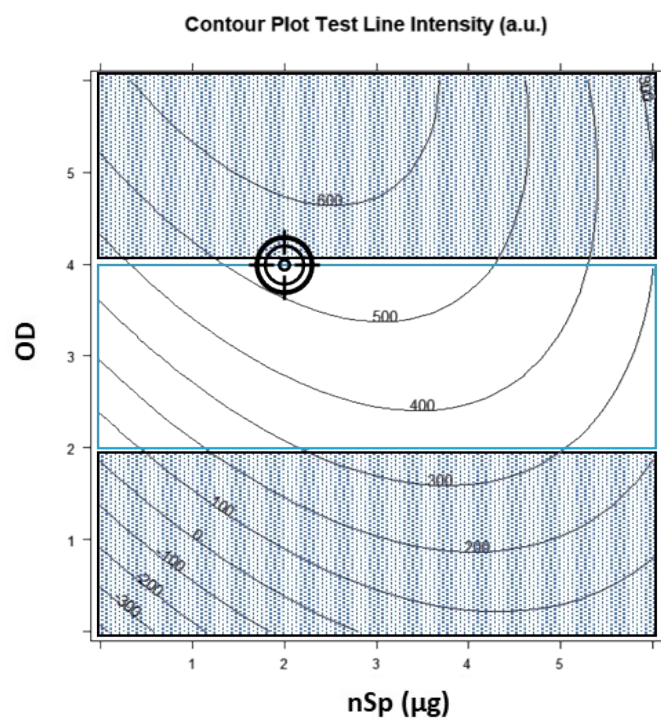
148

149 **Figure S9:** The results from the design of experiments for the decision on the gold conjugates parameters
 150 (protein and optical density) for the recombinant RBD (a), the SpA (b), and the anti-human IgG antibody (c).
 151 The bull's-eye refers to the probe chosen for the development of the LFIA devices. Blue shaded zones are
 152 unexplored experimental space.

153

154

155

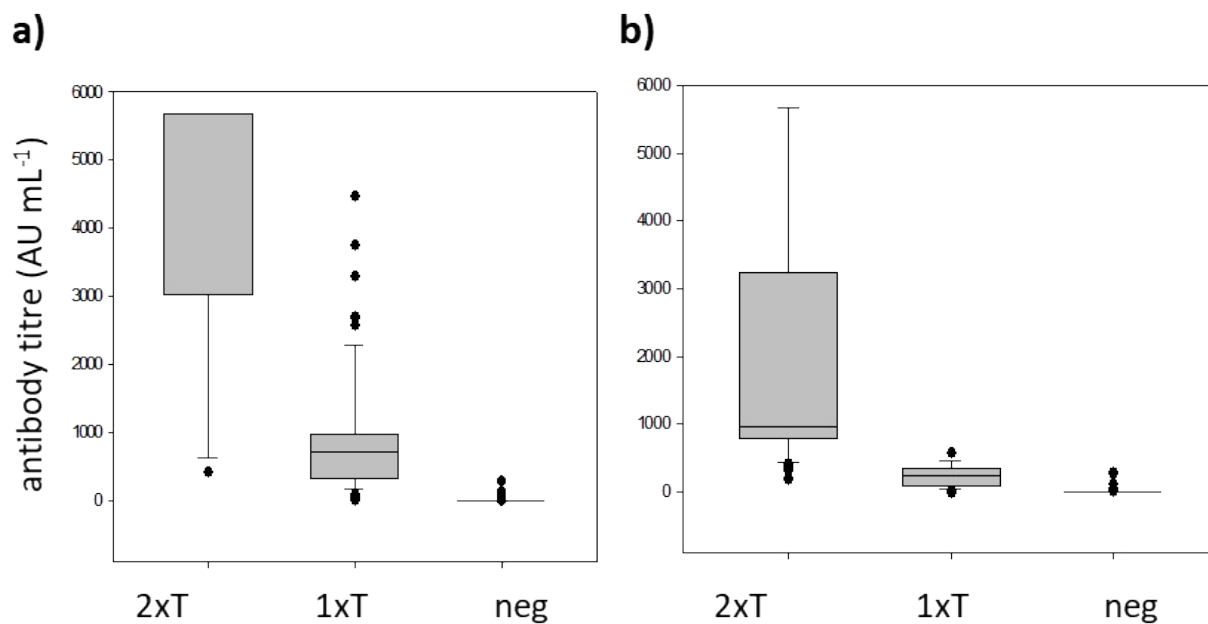


156

157 **Figure S10:** The results from the design of experiments for the decision on the gold conjugates parameters
158 (protein and optical density) for the new recombinant RBD. The bull's-eye refers to the probe chosen for the
159 development of the LFIA devices. Blue shaded zones are unexplored experimental space.

160

161

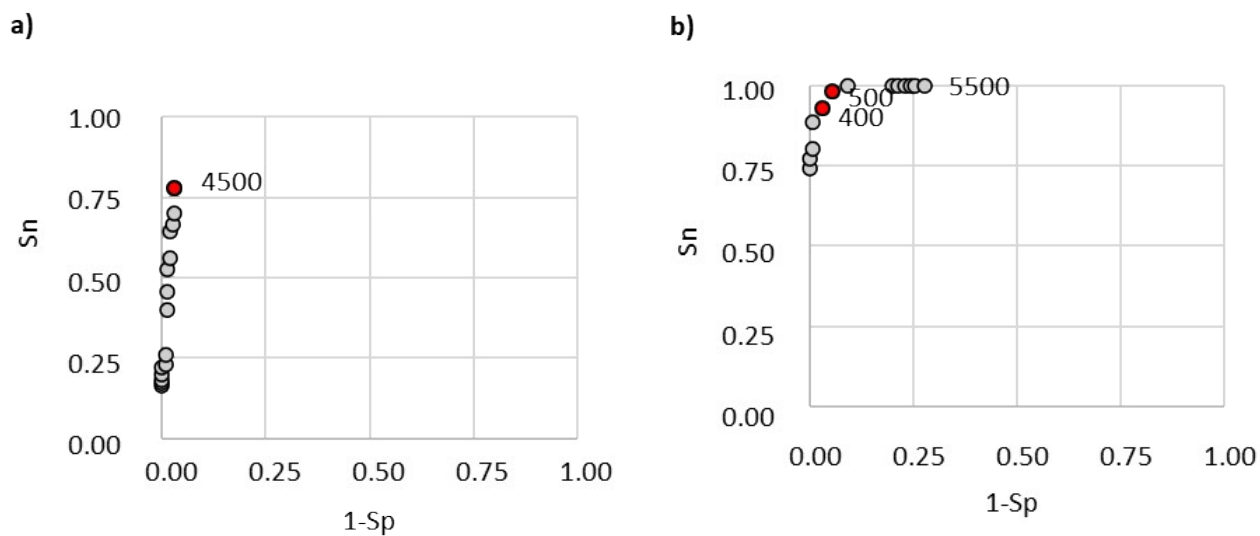


162

163 **Figure S11:** The Boxplot in a) represents the classification of the 171 samples provided by the
164 semiquantitative LFIA prototype including the new prepared recombinant RBD. The two test lines were
165 formed by the same recombinant RBD used as detector and were spotted at 1 mg mL⁻¹ in the first test line.
166 The second test line was spotted with 0.1 mg mL⁻¹ (a), and 0.25 mg mL⁻¹ (b).

167

168



169

170 **Figure S12:** ROC curves for the sqLFIA including the newly produced RBD (a) and the prototype including the
171 new RBD and in which the concentration of the capture protein on the second test line was increased from
172 0.1 to 0.25 mg mL⁻¹ (b). The red dots represent the estimation of the discrimination value of antibody titre
173 (AU mL⁻¹) that enabled the best classification of serum samples.

174

175

176

177

178 **TABLES**

179 **Table S1:** LSPR peaks from Visible spectra of the gold conjugates used in the DoE and in the LFIA-1, LFIA-2,
 180 and LFIA-3 devices.

Gold conjugate	Protein (μg)	λ_{max} LSPR (nm)	λ_{max} LSPR shift* (nm)
AuNP-cSp	1	526.1	1.1
	2	527.0	2.0
	4	527.9	2.9
AuNP-SpA	0.2	525.1	0.1
	0.5	525.5	0.5
	1	525.7	0.7
	2	526.1	1.1
	4	526.4	1.4
	6	526.4	1.4
	AuNP-anti-human IgG	5	530.4
	10	531.6	6.6
	15	531.9	6.9

181 * λ_{max} LSPR of the conjugate – λ_{max} LSPR of the bare AuNP

182

183

184 **Table S2:** Summary of the results obtained from the experimental design session for the optimization of the
185 parameters (protein-to-AuNP and optical density)

Gold conjugate	Protein x OD (levels)	FF-DoE (n of experiments)	D-optimal (n of experiments)	Explained variance (EV%)	Optimal gold conjugate (μ g; OD)
AuNP-cSp	3x3	9	-	96.91	1;4
AuNP-SpA	4x4	16	9	52.81	4;9
	3x3	9	-	92.29	
AuNP-anti-hIgG	3x3	9	-	84.15	15;6
	2x2	4	-	-	

186

187

188

189

190 **Table S3:** Study of the concentration of the second test line (T2) based on the ability of the multi lines LFIA
 191 to classify the high- (#1001), medium-high- (#1010), medium-low- (#1048), and low- (#1050) titre samples
 192 according to their antibody content. The conditions selected for further studies are highlighted in bold.

sqLFIA format	Concentration of T2 (mg mL ⁻¹)	Sample			
		High #1001	Medium-high #1010	Medium-low #1048	Low #1050
LFIA-1 (cSp)	1.0	+	+	+	+
	0.5	+	+	+	+
	0.25	+	+	+	+/-
	0.1	+	+	+/-	-
LFIA-2 (SpA)	1.0	+	+	+	+/-
	0.5	+	+	+	+/-
	0.25	+	+	+	+/-
	0.1	+/-	+/-	+/-	+/-

193 + clearly visible; +/- barely visible; - not visible

194

195

196

Table S4: Results from the three-test-line sqLFIA prototype for the 171 serum samples. The number of coloured test lines (3xT, 2xT, 1xT, neg) were clustered and analysed for their distribution by means of a Kruskal-Wallis One Way Analysis of Variance on Ranks, and the significance of the differences by Mann-Whitney method for Pairwise Comparison Procedure.

	N	Median	25-75%	P (Mann-Withney)	
3xT	42	1343	814-3933	3xT vs 2xT	0.01
2xT	7	715	371-934	2xT vs 1xT	0.248
1xT	21	341	193-574	1xT vs neg	<0.01
neg	102	0	0		

197

198

199

200

201 **Table S5:** LSPR peak from Visible spectra of the gold conjugates used in the DoE and in the LFIA-1 format for
202 the new recombinant RBD.

Gold conjugate	Protein (μg)	λ_{max} LSPR (nm)	λ_{max} LSPR shift* (nm)
AuNP-nSp	1	526.0	1.0
	2	527.7	2.7
	4	528.6	3.6

203 * λ_{max} LSPR of the conjugate - λ_{max} LSPR of the bare AuNP

204

205

206 **Table S6:** Summary of the results obtained from the experimental design session for the optimization of the
207 parameters (protein-to-AuNP and optical density) for the new recombinant RBD.

Gold conjugate		Protein x OD	FF-DoE	D-optimal	Explained variance (EV%)	Resulting gold conjugate (μ g;OD)
AuNP-nSp	Single- epitope	3x3	9	-	93.34	2;4

208

209

210 **Table S7:** Study of the concentration of the second test line (T2) based on the ability of the multi lines LFIA
 211 produced with the new recombinant RBD to classify the high-(#1001), medium-high-(#1010), medium-low-
 212 (#1048), and low-(#1050) titre samples according to their antibody content. The conditions selected for
 213 further studies are highlighted in bold.

sqLFIA format	Concentration of T2 (mg mL ⁻¹)	Sample			
		High #1001	Medium-high #1010	Medium-low #1048	Low #1050
LFIA-1 (nSp)	1.0	+	+	+	+
	0.5	+	+	+	+
	0.25	+	+	+/-	-
	0.1	+	+/-	-	-

214 + clearly visible; +/- barely visible; - not visible

215

216 **Table S8:** Results from the semiquantitative LFIA devices including the commercial and newly produced
 217 recombinant RBD for the 171 serum samples. The number of coloured test lines (2xT, 1xT, neg) were
 218 clustered and analysed for their distribution by means of a Kruskal-Wallis One Way Analysis of Variance on
 219 Ranks, and the significance of the differences by Dunn's Method for All Pairwise Multiple Comparison
 220 Procedure.

Kruskal-Wallis One Way Analysis of Variance on Ranks

T2=0.1mg/mL			T2=0.25mg/mL		
N	Median	25-75%	N	Median	25-75%
14	5680	3017-5680	54	969	784-3253
59	715	327-974	19	238	90-341
98	0	0	98	0	0

All Pairwise Multiple Comparison Procedures (Dunn's Method)

Diff of Ranks	Q	P<0,05	Diff of Ranks	Q	P<0,05
30.173	2.05	No	94.154	11.222	Yes
109.337	7.73	Yes	35.363	2.678	Yes
79.164	9.704	Yes	58.792	4.737	Yes

221

222

223

224 **References**

- 225 [1] X. Xia, Domains and functions of spike protein in sars-cov-2 in the context of vaccine design, *Viruses*.
226 13 (2021) 1–16. <https://doi.org/10.3390/v13010109>.
- 227 [2] G. Rigi, S. Ghaedmohammadi, G. Ahmadian, W.O. Library, A comprehensive review on
228 staphylococcal protein A (SpA): Its production and applications, *Int. Union Biochem. Mol. Biol. Inc.*
229 66 (2019) 454–464. <https://doi.org/10.1002/bab.1742>.
- 230 [3] S. Cavalera, G. Pezzoni, S. Grazioli, E. Brocchi, S. Baselli, D. Lelli, B. Colitti, T. Serra, F. Di Nardo, M.
231 Chiarello, V. Testa, S. Rosati, C. Baggiani, L. Anfossi, Investigation of the “Antigen Hook Effect” in
232 Lateral Flow Sandwich Immunoassay: The Case of Lumpy Skin Disease Virus Detection, *Biosensors*.
233 12 (2022) 739. <https://doi.org/10.3390/BIOS12090739>.

234